

MOPSO Based Multi-Objective Robust H_2/H_∞ Vibration Control for Typical Engineering Equipment

Huang WEI^{1,3)}, Xu JIAN²⁾, Zhu DA-YONG^{1,3)},
Lu JIAN-WEI¹⁾, Lu KUN-LIN^{1,3)}, Hu MING-YI^{4,5)}

¹⁾ *Hefei University of Technology*

Tunxi Road 193, Hefei, Anhui Province, China
e-mail: huangweiac@126.com

²⁾ *China National Machinery Industry Corporation*

Danning Street 3, Haidian, Beijing, China

³⁾ *Anhui Provincial Laboratory of Civil Engineering and Materials*

Tunxi Road 193, Hefei, Anhui Province, China

⁴⁾ North Road 160 of Xisihuan Street, Haidian, Beijing, China

⁵⁾ Zhongguancun North Street, Haidian, Beijing, China

Vibration control is critically important for engineering equipment, and in modern industrial engineering active strategies with robust performance are often adopted. In traditional studies, a single-objective consideration is often taken into account when robust control is performed, while a simultaneous multi-criterial consideration is ignored. The study outlined in this paper focuses on typical equipment, namely machinery and sensitive equipment. Meanwhile, evaluation of robust performances based on feedback control is considered as the vibration control objective, and performance indexes using H_∞ and H_2 criterion are regarded as fitness functions. In addition, the latest intelligent algorithm – MOPSO (multi-objective particle swarm optimization) is used and the SPEA2 (strength Pareto evolutionary algorithm 2) is also introduced for comparison as a representative of evolution algorithm.

Numerical results show that the Pareto frontier of MOPSO is much smoother and more uniformly distributed than SPEA2, and even more important is that MOPSO can obtain a unique, global and optimal solution *gbest*, which can avoid having to select just one from a group of equivalent solutions. Finally, an analysis of factors which affect the norms is performed, and the numerical verification shows that the disturbance type (single input or multi input) can apparently affect the magnitude of norms, and this finding can provide a broader understanding of robust vibration control. This research proposes a novel multi-objective optimization strategy for robust vibration control, while the traditional approaches can and are still employed. In addition, advanced artificial intelligence plays an important role in vibration detection in engineering application.

Key words: multi-objective particle swarm optimization, robust performance index, engineering equipment, active vibration control, disturbance type.

1. INTRODUCTION

Modern industry is rapidly becoming high-tech and high-precision, and this is closely accompanied by a key technique of application and innovation of engineering equipment. Such equipment can be divided into two types, one including rotating, reciprocating, impacting and other machinery equipment, and the other mainly including ultra-precision equipment, e.g., for high-precision grinding, measuring, etc. Vibration control is critical and essential issue for the use of such equipment and solving vibration problems associated with this use can effectively reduce the severe force transmitted to the surrounding environment. It is also very important to keep sensitive equipment away from harmful surrounding vibration in order for it to maintain its normal work.

The passive method is the most basic way which does not require any external energy supply, and it is also the simplest method to perform vibration isolation [1–3]. However, passive design is difficult to be implemented for low frequency, and often requires a compromise between isolation performance and supported machinery alignment [4]. To overcome the shortcomings of passive methods, active control methods have recently emerged in research such as Sky-hook [5], LQR/LQG [6], and H_2/H_∞ [7], etc.

Active vibration control can usually be described as optimization of some performance of a specific controller, and closed-loop performance is often indexed as an objective function. It is worth mentioning that the performance requirements of the control system are often not single-some indicators even conflict with each other and then multi-objective control needs to be performed. H_2/H_∞ norms are closely connected with robust performances, H_∞ control does not depend on an exact model of a controlled object, in which the robust stability is mainly considered and other performances are neglected, By contrast, H_2 control can compensate this shortfall, and a multi-objective balance of H_2 and H_∞ performance is both very important and necessary for robust control.

In general, multi-objective robust controls are usually solved by linear matrix inequality (LMI)toolbox, but this method has many deficiencies. For example only one sub-optimal solution can be found, LMI is required to be a convex set, and the mathematical derivation is very complicated for practical application [8]. With the development of new intelligent algorithms solving multi-objective optimization is becoming simpler and more effective. For example, a genetic algorithm NSGA (non-dominated sorting genetic algorithm), which is based on solving sorting, can generate an optimal Pareto set [9]. Meanwhile, strength Pareto evolutionary algorithm (SPEA) based on clustering approach [10] and SPEA2 improved from SPEA [11] are proposed one after another. In [12], a novel multi-objective robust H_2/H_∞ hybrid controller based on genetic algorithm was proposed, and the main conclusion was that genetic algorithm could significantly

reduce the conservatism problem of the LMI method. In [13], an evolutionary algorithm (EA) was synthesized with a multi-objective H_2/H_∞ controller and this study confirmed that application of EA to design a multi-objective H_2/H_∞ controller was feasible.

Traditional gradient-based optimization requires computations of sensitivity factors and eigenvectors at the iteration process. This causes an essential computational burden and slow convergence. Moreover, there is no local criterion to decide whether a local solution is also the global solution. Thus, the conventional optimization methods using derivatives and gradients are generally not able to locate or identify the global optimum. However, for real-world applications, one is often content with a good solution, even if it is not the best one. Consequently, heuristic methods are widely used for the global optimization problem. A particle swarm optimization (PSO) algorithm was first proposed by EBERHART and KENNEDY [14], it is a novel population-based metaheuristic optimization algorithm that utilizes the swarm intelligence generated by the cooperation and competition between the particles in a swarm. This method has become a useful tool for engineering optimization. FARSHIDIANFAR *et al.* [15] used the PSO technique to design a H_∞ controller for typical machinery and sensitive equipment, and the numerical results showed that static output feedback controller using PSO algorithm and H_∞ criterion could reach perfect performance to reduce harmful vibrations and disturbances.

COELLO *et al.* [16] first proposed the multi-objective particle swarm optimization (MOPSO) algorithm, with the principal idea being that by determining the flying directions of particles with optimal Pareto sets and a set of non-dominated solutions in the global knowledge base found before, the particles flying directions can be guided. This would enable, finally, a unique, optimal and global solution to be obtained. MOPSO can overcome some disadvantages of traditional multi-objective methods (such as SPEA and SPEA2, etc), such as those where a desired solution must be selected from a group of equivalent solutions [17].

2. BRIEF INTRODUCTION TO MOPSO

In the PSO algorithm, the state of every particle can be described by a group of position and velocity vectors which respectively represent the possible solutions and movement directions in the search space. The global optimum can be obtained by finding the optimal solutions and updating the optimal neighbor solutions. The main steps of MOPSO are summarized as following:

Step 1: Initialize the population, compute the corresponding objective vectors of particles and add the non-inferior solutions to the external archive,

Step 2: Initialize the local optimum $pbest$ of particles and the global optimum $gbest$,

Step 3: Adjust the velocities and positions of the particles by evaluating the following equations so as to generate a new $pbest$:

$$(2.1) \quad \mathbf{v}_{ij}(t+1) = \omega \mathbf{v}_{ij}(t) + c_1 r_1 (pbest_{ij}(t) - \mathbf{x}_{ij}(t)) + c_2 r_2 (gbest_{ij}(t) - \mathbf{x}_{ij}(t)),$$

$$(2.2) \quad \mathbf{x}_{ij}(t+1) = \mathbf{x}_{ij}(t) + \mathbf{v}_{ij}(t+1),$$

where i represents the i -th particle, j represents the j -th dimension of each particle, $\mathbf{v}_{ij}(t)$ represents the flight velocity component of j -th dimension of particles, $\mathbf{x}_{ij}(t)$ represents the flight displacement component of the $pbest$ -th dimension in the t -th generation, $pbest$ represents the local optimum, $gbest$ represents the global optimum, c_1 , c_2 are learning factors, r_1 , r_2 are random numbers between $(0, 1)$ and ω is the inertia weight factor, which plays a key role in the PSO,

Step 4: Maintain the external archive with the newly obtained non-inferior solution, and select $gbest$ for every and each particle (the archive determines the selection of global optimum),

Step 5: Check whether the maximum iteration has been reached, if not, the program will continue; if yes, terminate the computation and determine the optimal *Pareto* solution set and the $gbest$.

It is important to point out that direct computation will generate a set of equivalent solutions when traditional multi-objective optimization is performed, and it is difficult to determine the desired one. Pareto domination is the most direct way to solve this problem, namely this is conducted by considering all of the non-inferior solutions in the archive and determining a ‘leader’. The density measuring technique is then commonly used to determine the global optimum. The nearest neighbor density estimation method [9] based on nearest neighbor congestion evaluation is adopted in this paper. Certainly, there are also other similar methods, such as kernel density estimation method [18], etc.

3. BRIEF INTRODUCTION TO H_2/H_∞ CONTROLLER

Consider the feedback control system shown in Fig. 1.

Suppose the state-space form of the controlled system as

$$(3.1) \quad \begin{aligned} \dot{\mathbf{z}} &= \mathbf{A}\mathbf{z} + \mathbf{B}_1\mathbf{w} + \mathbf{B}_2u, \\ \mathbf{Y}_\infty &= \mathbf{C}_{\infty,1}\mathbf{z} + \mathbf{D}_{\infty,11}\mathbf{w} + \mathbf{D}_{\infty,12}u, \\ \mathbf{Y}_2 &= \mathbf{C}_{2,1}\mathbf{z} + \mathbf{D}_{2,11}\mathbf{w} + \mathbf{D}_{2,12}u, \\ \mathbf{y} &= \mathbf{C}_2\mathbf{z} + \mathbf{D}_{21}\mathbf{w} + \mathbf{D}_{22}u. \end{aligned}$$

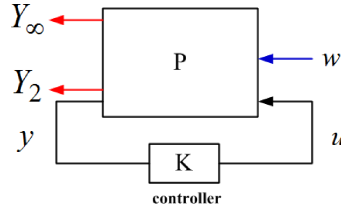


FIG. 1. Schematic of typical state-feedback controller.

In Eq. (3.1), \mathbf{z} is the state variable, \mathbf{w} is the input disturbance to the plant, \mathbf{Y}_∞ is the H_∞ performance, \mathbf{Y}_2 is the H_2 performance, \mathbf{y} is the observer's output, \mathbf{K} is the feedback controller, u is the output of controller (u is the control force generated by actuator in vibration control system, and $u = \mathbf{K}\mathbf{y}$), and P is the controlled plant.

In H_2/H_∞ control, a controller \mathbf{K} which makes the closed-loop system asymptotically stable is designed, namely the ∞ -norm of T_{wY} from \mathbf{w} to \mathbf{Y} is limited so as to ensure the robust stability; simultaneously, the designed \mathbf{K} should make the 2-norm of T_{wY} as low as possible.

Equation (3.1), to be solved, is usually divided into two steps and the first step can be expressed as

H_∞ performance:

min γ_1 s.t.

$$(3.2) \quad \begin{bmatrix} (\mathbf{A} + \mathbf{B}_2\mathbf{K})\mathbf{X}_\infty + \mathbf{X}_\infty(\mathbf{A} + \mathbf{B}_2\mathbf{K})^T & \mathbf{B}_1 & \mathbf{X}_\infty(\mathbf{C}_{\infty,1} + \mathbf{D}_{\infty,12}\mathbf{K})^T \\ \mathbf{B}_1^T & -\mathbf{I} & \mathbf{D}_{\infty,11}^T \\ (\mathbf{C}_{\infty,1} + \mathbf{D}_{\infty,12}\mathbf{K})\mathbf{X}_\infty & \mathbf{D}_{\infty,11} & -\gamma_1^2\mathbf{I} \end{bmatrix} < 0,$$

$$\mathbf{X}_\infty > 0.$$

The second step is

H_2 performance:

min \sqrt{v} such that

$$(3.3) \quad \begin{bmatrix} (\mathbf{A} + \mathbf{B}_2\mathbf{K})\mathbf{X}_2 + \mathbf{X}_2(\mathbf{A} + \mathbf{B}_2\mathbf{K})^T & \mathbf{B}_1 \\ \mathbf{B}_1^T & -\mathbf{I} \end{bmatrix} < 0,$$

$$\begin{bmatrix} \mathbf{Q} & (\mathbf{C}_{2,2} + \mathbf{D}_{2,22}\mathbf{K})\mathbf{X}_2 \\ \mathbf{X}_2(\mathbf{C}_{2,2} + \mathbf{D}_{2,22}\mathbf{K})^T & \mathbf{X}_2 \end{bmatrix} > 0,$$

$$\text{Trace}(\mathbf{Q}) < v^2,$$

$$\mathbf{X}_2 > 0, \quad \mathbf{Q} > 0.$$

4. H_2/H_∞ VIBRATION CONTROL FOR TYPICAL ENGINEERING EQUIPMENT

4.1. Machinery equipment

Consider the vibration control model of typical machinery equipment shown in Fig. 2.

a) Industrial machinery equipment



b) Model description

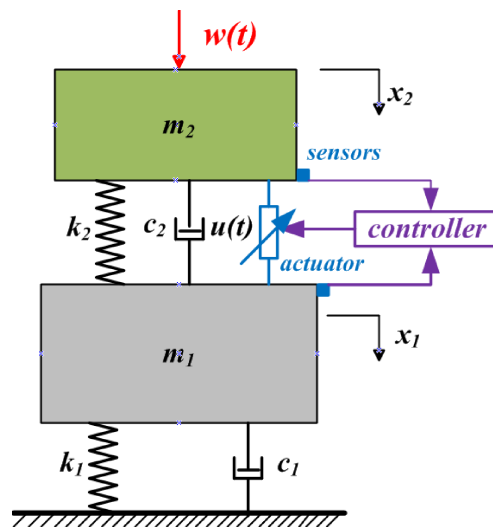


FIG. 2. Active vibration control of typical machinery equipment.

In Fig. 2, m_1, k_1, c_1 are respectively the mass, stiffness and damping of foundation or supporting structure, k_2, c_2 are respectively the stiffness and damping of isolation system, m_2 is the mass of machinery equipment, $u(t)$ is the control force generated by actuator, $w(t)$ is the dynamic disturbance generated by the machinery equipment, which is denoted as $w(t) = F \sin(\omega t)$. The motion equations can be written as

$$(4.1) \quad \begin{aligned} m_1 \ddot{x}_1 + k_1 x_1 + c_1 \dot{x}_1 - c_2(\dot{x}_2 - \dot{x}_1) - k_2(x_2 - x_1) &= u(t), \\ m_2 \ddot{x}_2 + c_2(\dot{x}_2 - \dot{x}_1) + k_2(x_2 - x_1) &= w(t) - u(t). \end{aligned}$$

Suppose the state variables as $x_1 = z_1, x_2 = z_2, \dot{x}_1 = z_3, \dot{x}_2 = z_4, \mathbf{z} = [z_1, z_2, z_3, z_4]^T$, then Eq. (4.1) can be rewritten as the state-space form:

$$(4.2) \quad \dot{\mathbf{z}} = \mathbf{A}\mathbf{z} + \mathbf{B}_1\mathbf{w} + \mathbf{B}_2u,$$

$$\mathbf{A} = \begin{bmatrix} 0 & 0 & 1 & 0 \\ 0 & 0 & 0 & 1 \\ -\frac{k_1 + k_2}{m_1} & \frac{k_2}{m_1} & -\frac{c_1 + c_2}{m_1} & \frac{c_2}{m_1} \\ \frac{k_2}{m_2} & -\frac{k_2}{m_2} & \frac{c_2}{m_2} & -\frac{c_2}{m_2} \end{bmatrix},$$

$$\mathbf{B}_1 = \begin{bmatrix} 0 \\ 0 \\ 0 \\ \frac{1}{m_2} \end{bmatrix}, \quad \mathbf{B}_2 = \begin{bmatrix} 0 \\ 0 \\ -\frac{1}{m_1} \\ \frac{1}{m_2} \end{bmatrix}.$$

Suppose the H_∞ output of the given system as

$$(4.3) \quad \mathbf{Y}_\infty = [k_1 x_1 + c_1 \dot{x}_1, x_1, \ddot{x}_1, x_2 - x_1, \ddot{x}_2]^T.$$

Then, Eq. (4.3) can be rewritten as the state-space form:

$$(4.4) \quad \mathbf{Y}_\infty = \mathbf{C}_{\infty,1}\mathbf{z} + \mathbf{D}_{\infty,11}\mathbf{w} + \mathbf{D}_{\infty,12}u,$$

$$\mathbf{C}_{\infty,1} = \begin{bmatrix} k_1 & 0 & c_1 & 0 \\ 1 & 0 & 0 & 0 \\ -\frac{k_1+k_2}{m_1} & \frac{k_2}{m_1} & -\frac{c_1+c_2}{m_1} & \frac{c_2}{m_1} \\ 1 & -1 & 0 & 0 \\ \frac{k_2}{m_2} & -\frac{k_2}{m_2} & \frac{c_2}{m_2} & -\frac{c_2}{m_2} \end{bmatrix},$$

$$\mathbf{D}_{\infty,11} = \begin{bmatrix} 0 \\ 0 \\ 0 \\ 0 \\ \frac{1}{m_2} \end{bmatrix}, \quad \mathbf{D}_{\infty,12} = \begin{bmatrix} 0 \\ 0 \\ \frac{1}{m_1} \\ 0 \\ -\frac{1}{m_2} \end{bmatrix}.$$

For convenience, the H_2 output is assumed to be the same as the H_∞ output in this paper, i.e., $\mathbf{Y}_2 = \mathbf{Y}_\infty$.

Set the observed output as $\mathbf{y} = [x_2 - x_1, \dot{x}_1]^T$ and the state-space form can be written as

$$(4.5) \quad \mathbf{y} = \mathbf{C}_2 \mathbf{z} + \mathbf{D}_{21} \mathbf{w} + \mathbf{D}_{22} u,$$

$$\mathbf{C}_2 = \begin{bmatrix} -1 & 1 & 0 & 0 \\ 0 & 0 & 1 & 0 \end{bmatrix}, \quad \mathbf{D}_{21} = \begin{bmatrix} 0 \\ 0 \end{bmatrix}, \quad \mathbf{D}_{22} = \begin{bmatrix} 0 \\ 0 \end{bmatrix}.$$

According to [15], the closed-loop transfer function with respect to \mathbf{Y}_∞ performance index can be derived as

$$(4.6) \quad \mathbf{T}_{\mathbf{wY}_\infty} = \mathbf{D}_{\text{cl}} + \mathbf{C}_{\text{cl}}(s\mathbf{I}_2 - \mathbf{A}_{\text{cl}})^{-1}\mathbf{B}_{\text{cl}},$$

$$\mathbf{A}_{\text{cl}} = \mathbf{A} + \mathbf{B}_2 \mathbf{K}(\mathbf{I}_1 - \mathbf{D}_{22} \mathbf{K})^{-1} \mathbf{C}_2, \quad \mathbf{B}_{\text{cl}} = \mathbf{B}_1 + \mathbf{B}_2 \mathbf{K}(\mathbf{I}_1 - \mathbf{D}_{22} \mathbf{K})^{-1} \mathbf{D}_{21},$$

$$\mathbf{C}_{\text{cl}} = \mathbf{C}_{\infty,1} + \mathbf{D}_{\infty,12} \mathbf{K}(\mathbf{I}_1 - \mathbf{D}_{\infty,22} \mathbf{K})^{-1} \mathbf{C}_2,$$

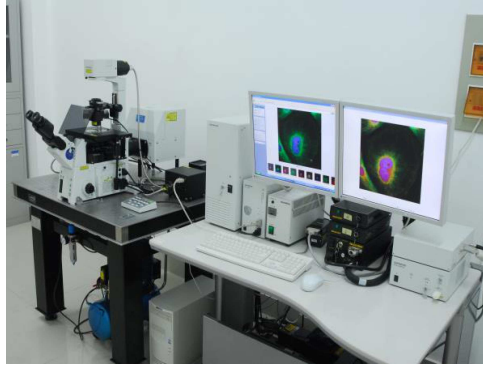
$$\mathbf{D}_{\text{cl}} = \mathbf{D}_{\infty,11} + \mathbf{D}_{\infty,12} \mathbf{K}(\mathbf{I}_1 - \mathbf{D}_{22})^{-1} \mathbf{D}_{21},$$

\mathbf{I}_1 , \mathbf{I}_2 are identity matrices, $s = j\omega$ is the Laplace operator and ω is the circular frequency.

4.2. Sensitive equipment

Consider the vibration control model of typical sensitive equipment shown in Fig. 3.

a) Sensitive equipment



b) Model description

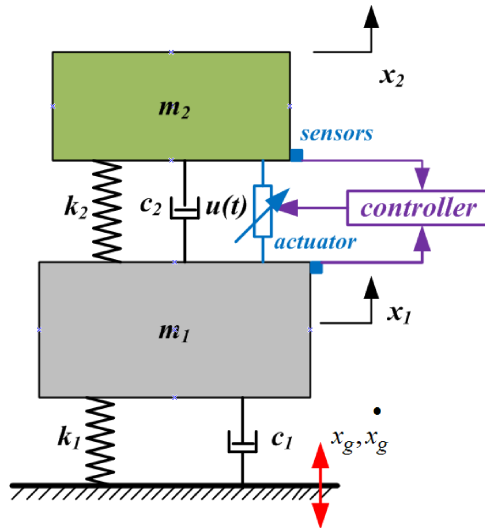


FIG. 3. Active vibration control of typical sensitive equipment.

At present, the input disturbance is considered as the ground disturbance, which can be referred to as $\mathbf{w}(t) = [x_g, \dot{x}_g]^T$ and the other parameters are consistent with the aforementioned machinery model. The motion equation can be written as

$$(4.7) \quad \begin{aligned} m_1 \ddot{x}_1 - c_2 \dot{x}_2 + (c_1 + c_2) \dot{x}_1 - k_2 x_2 + (k_1 + k_2) x_1 &= c_1 \dot{x}_g + k_1 x_g - u(t), \\ m_2 \ddot{x}_2 + c_2 (\dot{x}_2 - \dot{x}_1) + k_2 (x_2 - x_1) &= u(t). \end{aligned}$$

Similarly, the state variables are set as $x_1 = z_1$, $x_2 = z_2$, $\dot{x}_1 = z_3$, $\dot{x}_2 = z_4$, $\mathbf{z} = [z_1, z_2, z_3, z_4]^T$, then Eq. (4.7) can be rewritten as the state-space form:

$$(4.8) \quad \dot{\mathbf{z}} = \mathbf{A}\mathbf{z} + \mathbf{B}_1\mathbf{w} + \mathbf{B}_2u,$$

$$\mathbf{A} = \begin{bmatrix} 0 & 0 & 1 & 0 \\ 0 & 0 & 0 & 1 \\ \frac{k_1 + k_2}{m_1} & -\frac{k_2}{m_1} & \frac{c_1 + c_2}{m_1} & -\frac{c_2}{m_1} \\ \frac{k_2}{m_2} & -\frac{k_2}{m_2} & \frac{c_2}{m_2} & -\frac{c_2}{m_2} \end{bmatrix},$$

$$\mathbf{B}_1 = \begin{bmatrix} 0 & 0 \\ 0 & 0 \\ \frac{k_1}{m_1} & \frac{c_1}{m_1} \\ 0 & 0 \end{bmatrix}, \quad \mathbf{B}_2 = \begin{bmatrix} 0 \\ 0 \\ -\frac{1}{m_1} \\ \frac{1}{m_2} \end{bmatrix}.$$

For now, the H_∞ output can be assumed as

$$(4.9) \quad Y_\infty = [x_2, \dot{x}_2]^T.$$

Equation (4.9) can be rewritten in state-space form as

$$(4.10) \quad \mathbf{Y}_\infty = \mathbf{C}_{\infty,1}\mathbf{z} + \mathbf{D}_{\infty,11}\mathbf{w} + \mathbf{D}_{\infty,12}u,$$

$$\mathbf{C}_{\infty,1} = \begin{bmatrix} 0 & 0 & 1 & 0 \\ 0 & 0 & 0 & 1 \end{bmatrix}, \quad \mathbf{D}_{\infty,11} = \begin{bmatrix} 0 & 0 \\ 0 & 0 \end{bmatrix}, \quad \mathbf{D}_{\infty,12} = \begin{bmatrix} 0 \\ 0 \end{bmatrix}.$$

Likewise, the H_2 output is supposed to be the same as the H_∞ output.

Set the observed output as $y = [x_2 - x_1, \dot{x}_1]^T$, and the state-space form can be written as

$$(4.11) \quad \mathbf{y} = \mathbf{C}_2\mathbf{z} + \mathbf{D}_{21}\mathbf{w} + \mathbf{D}_{22}u,$$

$$\mathbf{C}_2 = \begin{bmatrix} -1 & 1 & 0 & 0 \\ 0 & 0 & 1 & 0 \end{bmatrix}, \quad \mathbf{D}_{21} = \begin{bmatrix} 0 \\ 0 \end{bmatrix}, \quad \mathbf{D}_{22} = \begin{bmatrix} 0 \\ 0 \end{bmatrix}.$$

The closed-loop transfer function with reference to Y_∞ performance index can be derived as

$$(4.12) \quad \mathbf{T}_{\mathbf{w}Y_\infty} = \mathbf{D}_{cl} + \mathbf{C}_{cl}(s\mathbf{I}_2 - \mathbf{A}_{cl})^{-1}\mathbf{B}_{cl},$$

$$\mathbf{A}_{cl} = \mathbf{A} + \mathbf{B}_2\mathbf{K}(\mathbf{I}_1 - \mathbf{D}_{22}\mathbf{K})^{-1}\mathbf{C}_2, \quad \mathbf{B}_{cl} = \mathbf{B}_1 + \mathbf{B}_2\mathbf{K}(\mathbf{I}_1 - \mathbf{D}_{22}\mathbf{K})^{-1}\mathbf{D}_{21},$$

$$\mathbf{C}_{cl} = \mathbf{C}_{\infty,1} + \mathbf{D}_{\infty,12}\mathbf{K}(\mathbf{I}_1 - \mathbf{D}_{\infty,22}\mathbf{K})^{-1}\mathbf{C}_2,$$

$$\mathbf{D}_{cl} = \mathbf{D}_{\infty,11} + \mathbf{D}_{\infty,12}\mathbf{K}(\mathbf{I}_1 - \mathbf{D}_{22})^{-1}\mathbf{D}_{21}.$$

5. NUMERICAL STUDIES

For the two models of active vibration control, the MOPSO technique is used to optimize the H_2/H_∞ norms for the purpose of obtaining the optimal feedback controller. The *fitness* functions are defined as

$$(5.1) \quad \begin{aligned} fitness_1 &= \|\mathbf{T}\mathbf{w}\mathbf{Y}_\infty\|_\infty, \\ fitness_2 &= \|\mathbf{T}\mathbf{w}\mathbf{Y}_2\|_2, \end{aligned}$$

Parameter settings of the two vibration isolation systems are presented in Table 1 [15].

Table 1. Given parameters of the simulation equipment models.

Machinery equipment model	Sensitive equipment model
	$m_1 = 560$ kg
$m_2 = 560$ kg	$m_2 = 100$ kg
$k_1 = 2.5 \times 10^5$ N/m	$k_1 = 1.5 \times 10^5$ N/m
$k_2 = 1.5 \times 10^4$ N/m	$k_2 = 2.5 \times 10^4$ N/m
$c_1 = 100$ N/ms ⁻¹	$c_1 = 100$ N/ms ⁻¹
$c_2 = 10$ N/ms ⁻¹	$c_2 = 10$ N/ms ⁻¹

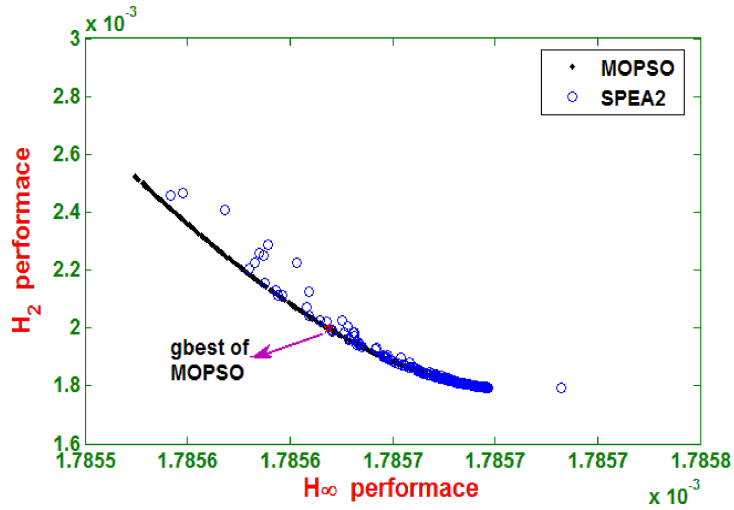
For comparison, the SPEA2 is introduced as a representative of typical evolutionary algorithms. Parameters of MOPSO are arbitrarily set as following: population size is 200, maximum iteration is 200, inertia weight coefficients are $\omega_{\max} = 0.9$, $\omega_{\min} = 0.4$ and the learning factors are $c_1 = 2$, $c_2 = 2$.

The parameters of SPEA2 are arbitrarily set as following: population size is 200, maximum iteration is 200, the generation number of mate selection tournament is 2, individual mutation probability is 1, individual recombination probability is 1, variable mutation probability is 1, variable exchange probability is 0.5 and the variable recombination probability is 1.

The searching range of feedback controller \mathbf{K} is configured as $[-1 \times 10^5, 1 \times 10^5]$.

Apparently, as seen in Fig. 4, Pareto frontiers based on MOPSO are much smoother and more uniformly distributed, and parameters settings of MOPSO are quite convenient contrary to SPEA2. In addition, the MOPSO based optimization can obtain a unique *gbest* solution which can make the computation more convenient and reliable. The SPEA2, however, generates a set of equivalent Pareto solutions and a desired solution must be selected by the use of a certain rule. In view of the above, optimal controllers generated by MOPSO are listed in Table 2.

a) Pareto frontiers for comparison (machinery equipment model)



b) Pareto frontiers for comparison (sensitive equipment model)

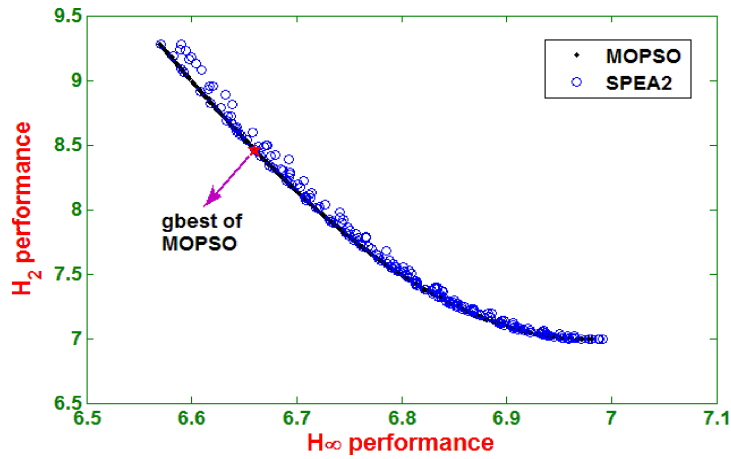


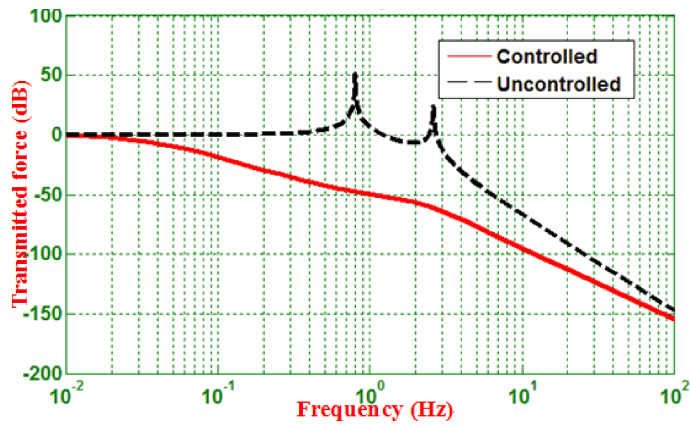
FIG. 4. Pareto frontiers of the two models by MOPSO and SPEA2.

Table 2. Obtained optimal feedback controller by MOPSO.

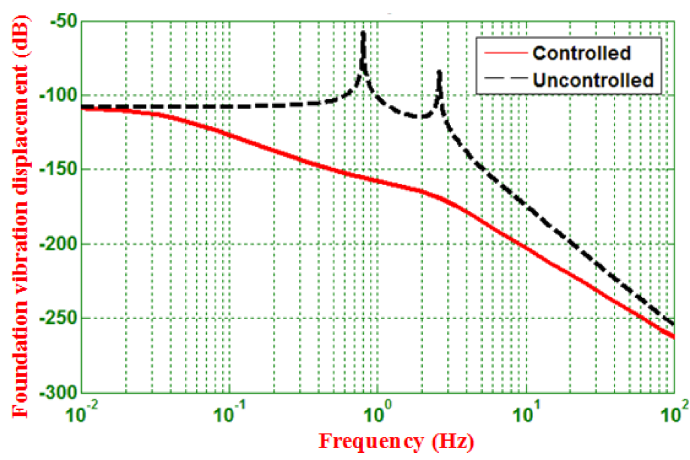
Machinery equipment model	Sensitive equipment model
$\mathbf{K} = [-1.5028, -1.9034] \times 10^4$	$\mathbf{K} = [1.3371, -0.003649] \times 10^4$

As shown in Figs. 5, 6, the MOPSO based H_2/H_∞ controller can effectively reduce the undesired vibration of the typical equipment. So far, the multi-objective design of H_2/H_∞ controller is effectively solved.

a) force transmitted to the foundation



b) foundation vibration displacement



c) foundation vibration acceleration

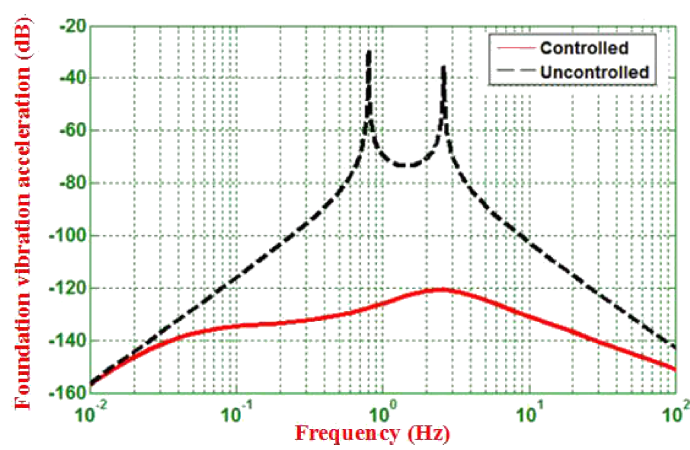
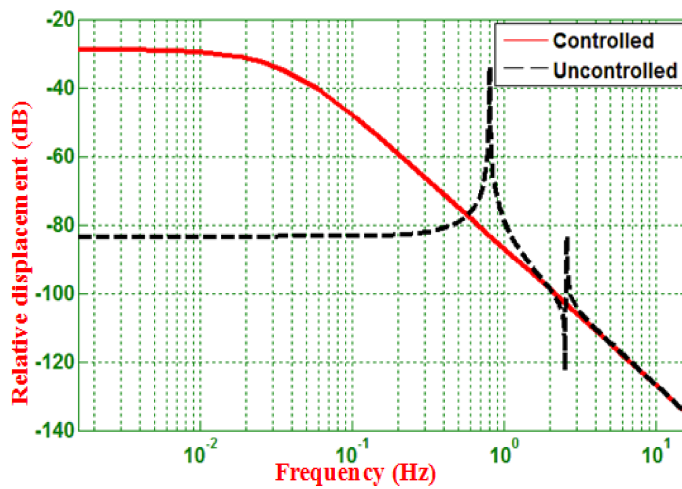


[FIG. 5a,b,c]

d) relative displacement



e) machinery equipment acceleration

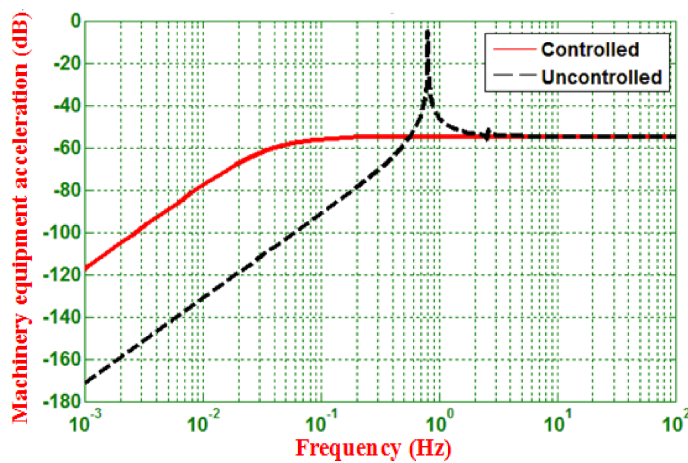
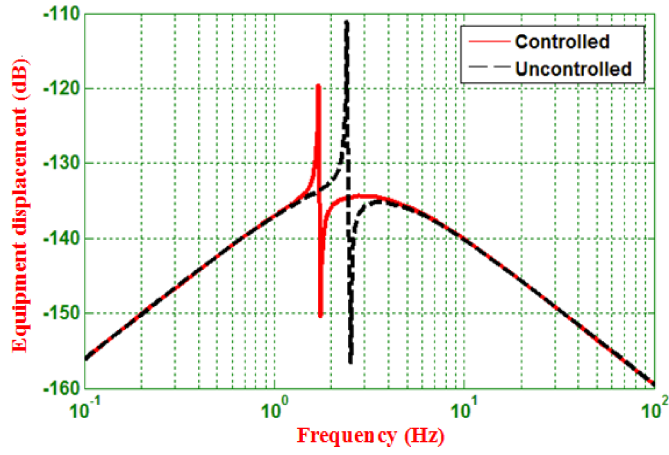


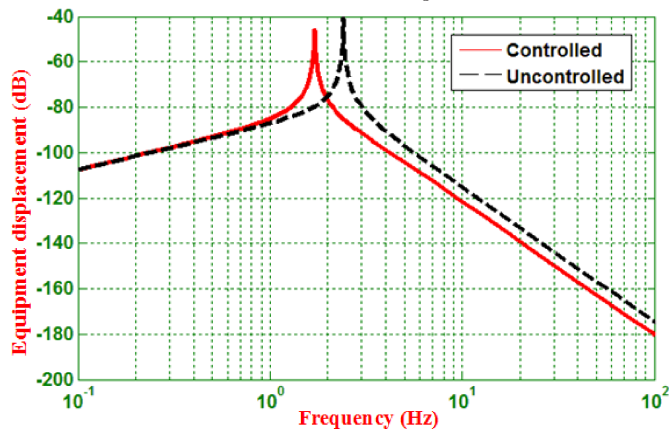
FIG. 5. Controlled output with optimal feedback controller vs. uncontrolled condition (machinery equipment).

In addition, a phenomenon in this paper should be pointed out for further study. As seen in Fig. 5, the H_2/H_∞ criterion of the machinery equipment model excited by the single-input has a larger difference of magnitude than the sensitive equipment excited by the double-input type (denoted as $w(t) = [x_g, x_g]^T$), and this may indicate that some factors can affect it more than others. To perform further analysis, an influence of isolation parameters will be considered first and the updated parameters are listed in Table 3 [15].

a) equipment displacement (input x_g to output x_2)



b) equipment displacement (input \dot{x}_g to output x_2)



c) equipment velocity (input x_g to output \dot{x}_2)

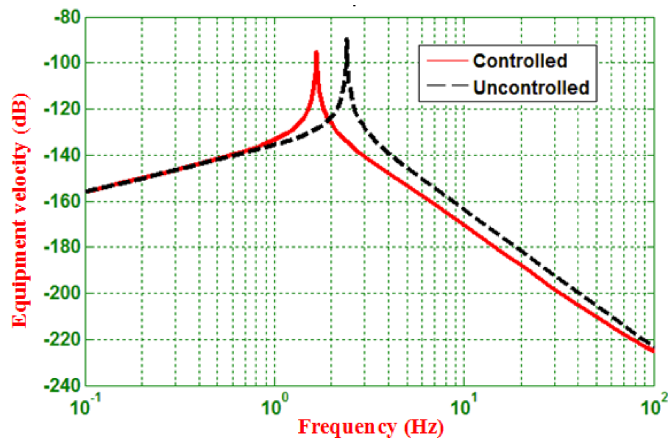


[FIG. 6a,b,c]

d) equipment velocity (input \dot{x}_g to output \dot{x}_2)

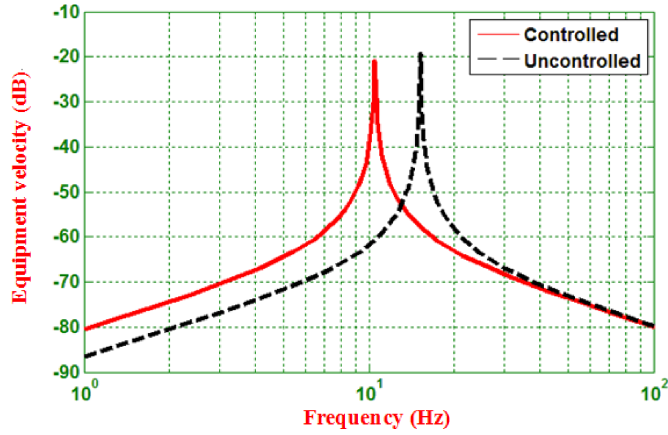


FIG. 6. Controlled output with optimal feedback controller vs. uncontrolled condition (sensitive equipment model).

Table 3. Isolation parameters variation of the double input system.

Sensitive equipment model (case 1)
$m_1 = 560$ kg
$m_2 = 10$ kg
$k_1 = 1.5 \times 10^5$ N/m
$k_2 = 2.5 \times 10^4$ N/m
$c_1 = 10$ N/ms ⁻¹
$c_2 = 100$ N/ms ⁻¹

As seen in Fig. 7, isolation parameters do not obviously affect the H_2/H_∞ performance. The second case is that the single-input disturbance is consid-

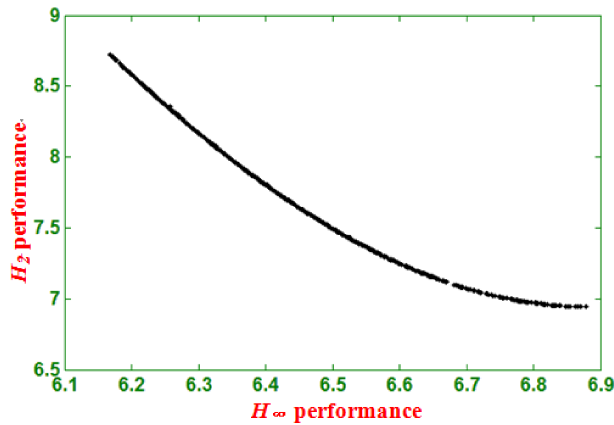


FIG. 7. Pareto frontier of case 1.

ered as a double-input type, and the excitation is regarded as a harmonic force F transmitted from the ground or surrounding environment (case 2).

Disturbance type will make the H_2/H_∞ norms undergo tremendous change and the magnitude can be even reduced to 10^{-5} , as it seen in Fig. 8. For specific vibration isolation systems, the actual input style may affect the controlled system much more than the isolation parameters. In other words, sensitive equipment should be kept away from some traffic- induced ground motions [19] which vibrate in the following form: $[x_g, \dot{x}_g]^T$.

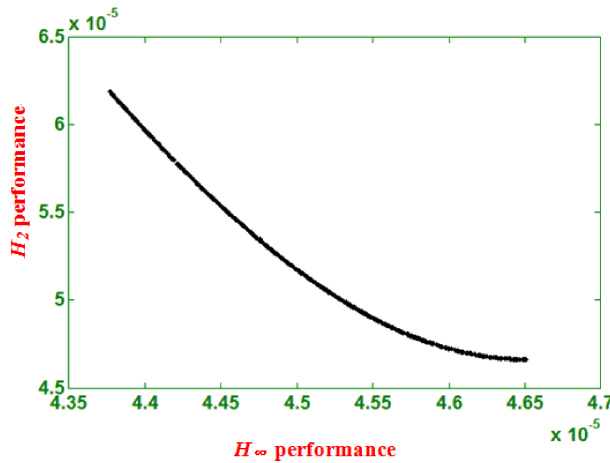


FIG. 8. Pareto frontier of case 2.

6. CONCLUSIONS

Multi-objective robust H_2/H_∞ active vibration control based on MOPSO technique for typical engineering equipment is presented in this paper and the numerical studies can confirm its effectiveness. The presented method can compensate a lot for typical H_∞ control (single-objective optimization), and the artificial intelligence algorithm adopted here allows to obtain a feedback controller.

It is worth mentioning that the H_2 performance is assumed in this paper, for convenience, to be the same as the H_∞ performance. In fact, these two performances should be treated seriously in practice, because they should exactly reflect the robustness. In addition, disturbance type is also validated as important for the controlled system when robust controller is performed.

This study can give strong inspiration for multi-objective robust vibration control of traditional engineering equipment; especially the application of artificial intelligence in this H_2/H_∞ problem may promote the traditional method.

ACKNOWLEDGMENT

This research was completely supported by the National Natural Science Foundation of China, and the Grants 51078123, 51179043. Valuable comments and suggestions offered by the experts on the national code of China “Code for Vibration Load Design of Industrial Buildings” are gratefully acknowledged by the authors.

REFERENCES

1. HARRIS C.M., *Shock and vibration handbook*, 33–50, McGraw-Hill, New York, 1987.
2. BEARD A.M., SCHUBERT D.W., VON FLOTOW A.H., *Practical product implementation of an active/passive vibration isolation system*, Proceedings of SPIE 1994 International Symposium on Optics, Imaging, and Instrumentation, International Society for Optics and Photonics, 38–49, 1994.
3. BRONOWICKI A.J., MACDONALD R., GURSEL Y., *Dual stage passive vibration isolation for optical interferometer missions*, Astronomical Telescopes and Instrumentation, International Society for Optics and Photonics, 753–763, 2003.
4. DALEY S., HÄTÖNEN J., OWENS D.H., *Active vibration isolation in a “smart spring” mount using a repetitive control approach*, Control Engineering Practice, **14**, 9, 991–997, 2006.
5. KARNOPP D., CROSBY M.J., HARWOOD R.A., *Vibration control using semi-active force generators*, Journal of Manufacturing Science and Engineering, **96**, 2, 619–626, 1974.
6. HROVAT D., *Applications of optimal control to advanced automotive suspension design*, Journal of Dynamic Systems, Measurement, and Control, **115**, 2, 328–342, 1993.
7. DU H., YIM SZE K., LAM J., *Semi-active H_∞ control of vehicle suspension with magnetorheological dampers*, Journal of Sound and Vibration, **283**, 3, 981–996, 2005.
8. BAEYENS E., KHARGONEKAR P.P., *Some examples in mixed H_2/H_∞ control*, American Control Conference, Vol. 2, 1608–1612, 1994.
9. DEB K., PRATAP A., AGARWAL S., MEYARIVAN T., *A fast and elitist multiobjective genetic algorithm: NSGA-II*, Evolutionary Computation, IEEE Transactions on Evolutionary Computation, **6**, 2, 182–197, 2002.
10. ZITZLER E., THIELE L., *Multiobjective evolutionary algorithms: a comparative case study and the strength Pareto approach*, Evolutionary Computation, **3**, 4, 257–271, 1999.
11. LAUMANN M., *SPEA2: Improving the strength Pareto evolutionary algorithm*, 19–26, 2001.
12. MOLINA-CRISTÓBAL A., GRIFFIN I.A., FLEMING P.J., *Linear matrix inequalities and evolutionary optimization in multiobjective control*, International Journal of Systems Science, **37**, 8, 513–522, 2006.
13. PEDERSEN G.K.M., LANGBALLE A.S., WISNIEWSKI R., *Synthesizing multi-objective H_2/H_∞ dynamic controller using evolutionary algorithms*, 15th Triennial World Congress, 2002.

14. EBERHART R.C., KENNEDY J., *A new optimizer using particle swarm theory*, Proceedings of the Sixth International Symposium on Micro Machine and Human Science, 39–42, 1995.
15. FARSHIDIANFAR A., SAGHAFI A., KALAMI S.M., SAGHAFI I., *Active vibration isolation of machinery and sensitive equipment using H_∞ control criterion and particle swarm optimization method*, Meccanica, **47**, 2, 437–453, 2012.
16. COELLO C.A., LECHUGA M.S., *MOPSO: A proposal for multiple objective particle swarm optimization*, Proceedings of the 2002 Congress on IEEE, 1051–1056, 2002.
17. FONSECA C.M., FLEMING P.J., *An overview of evolutionary algorithms in multi-objective optimization*, evolutionary computation, **3**, 1, 1–16, 1995.
18. GOLDBERG D.E., RICHARDSON J., *Genetic algorithms with sharing for multimodal function optimization*, Genetic Algorithms and their Applications: Proceedings of the Second International Conference on Genetic Algorithms, 41–49, 1987.
19. XU Y.L., YANG Z.C., CHEN J., LIU H.J., *Micro vibration control platform for high technology facilities subject to traffic-induced ground Motion*, Engineering Structures, **25**, 8, 1069–1082, 2003.

Received October 9, 2014; accepted April 8, 2015.
